Noname manuscript No.
(will be inserted by the editor)

Vapor-liquid steady meniscus at a superheated wall: asymptotics in an intermediate zone near the contact line

A. Ye. Rednikov · P. Colinet

Received: date / Accepted: date

Abstract The study concerns steady configurations of a perfectly wetting liquid in contact with its pure vapor and a superheated substrate/wall maintained at a constant temperature. Despite the perfect wetting, the system is characterized by a finite apparent contact angle formed at a microscale, within a steady microstructure of the contact line, the finiteness owing itself to an actually dynamic situation caused by the evaporation process. The angle is assumed to be small here, which is the case for sufficiently small superheats. When macroscopically treating a steady meniscus, one typically implies that the wall is met at the contact angle given by the microstructure. This remains somewhat an intuitive, heuristic approach unless a more rigorous asymptotic matching is carried out between the meniscus and the microstructure, which is accomplished in the present paper by studying an intermediate zone connecting these two regions. The analysis, based upon a standard one-sided planar model of an evaporating liquid layer in the lubrication approximation, confirms the validity of the mentioned approach. A possible uncertainty in the definition of the contact angle is shown to be small given that the macroscopic curvature (i.e. that of the meniscus and of the wall) is small on the scale of the contact line microstructure.

Keywords Contact line · Evaporation · Superheat · Thin film · Heat transfer · Asymptotics

A. Ye. Rednikov · P. Colinet
Université Libre de Bruxelles, TIPs-Fluid Physics, CP 165/67, 1050 Brussels, Belgium
Tel.: +322-6504096 and +322-6503561
Fax: +322-6502910
E-mail: aredniko@ulb.ac.be, pcolinet@ulb.ac.be

1 Introduction

Understanding of the processes occurring at a pure-vapor/liquid contact line on a (super)heated solid surface is of significant importance for modeling heat and mass transfer in evaporating systems. Examples of such systems include evaporating steady menisci at heated walls [1–3] and in particular those in grooved heat pipes [4, 5]. In the perfectly wetting case, the mentioned studies are concerned with, the contact line possesses quite a specific structure with well defined microscales (thus we refer to it as the microstructure) and whose noteworthy element is an adsorbed microfilm ([1] and subsequent studies) extending over the adjacent spots of the (smooth) solid surface unoccupied by macroscopic portions of the liquid (see figure 1). The microfilm is in thermodynamic equilibrium with the vapor at the temperature of the solid $T_w^* = T_0^* + \Delta T^*$, which is higher (superheat $\Delta T^* > 0$) than the saturation temperature $T_0^* = T_{sat}^*(p_0^*)$ corresponding to the vapor pressure p_0^*. This equilibrium is a result of the Kelvin effect as caused by the disjoining pressure. The disjoining pressure isotherm as a function of the film thickness ξ^* is here taken in the form $\Pi^*(\xi^*) = A^*/\xi^{*3}$ with $A^* > 0$ typical for non-polar liquids. Then, for small enough ΔT^*, the microfilm thickness is

$$\xi_f^* = \left(\frac{A^*\, T_0^*}{\mathcal{L}^*\, \rho_l^*\, \Delta T^*} \right)^{1/3} , \qquad (1)$$

where $\mathcal{L}^*$ is the latent heat of evaporation, ρ^* is the density. Hereafter the subscripts 'v' and 'l' refer to the vapor and the liquid, respectively.

The steady microstructure admits a film configuration asymptotically reaching a constant slope at infinity [4]. Within the macroscopic problem (of a steady meniscus), this slope is considered to correspond to the

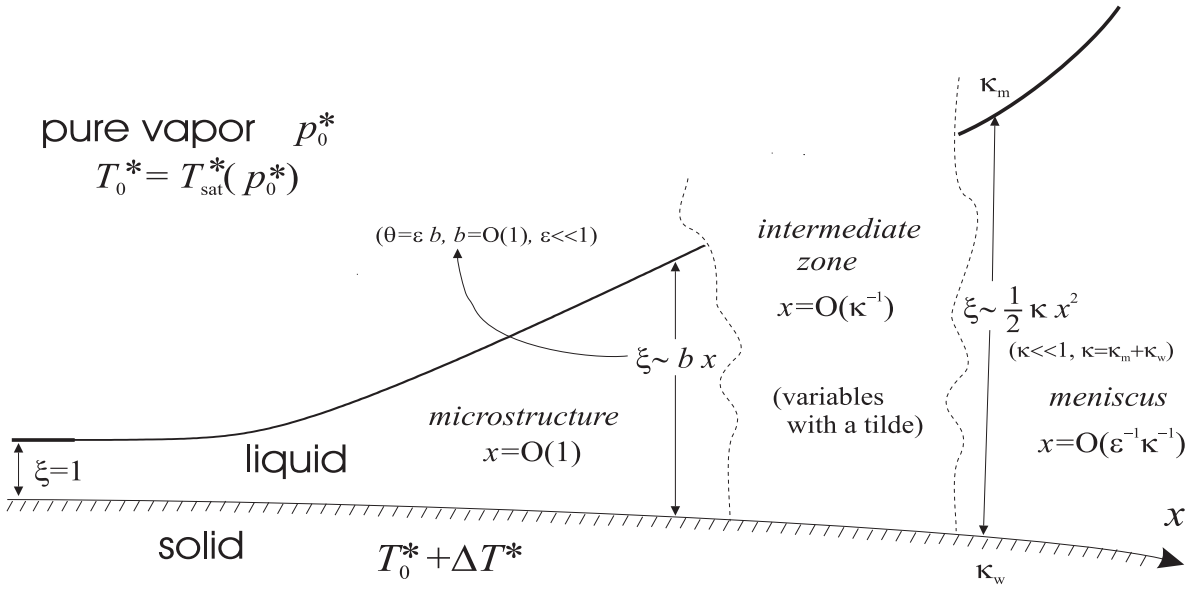

Fig. 1 Configuration sketch

apparent contact angle θ. For this approach to be valid, any uncertainty in the definition of the contact angle introduced due to a finite (but small on the microscale) macroscopic curvature must be small.

The present analysis, limited to a planar geometry, is concerned with building an asymptotic expansion describing the film behavior in an intermediate zone between the microstructure and the meniscus. In particular, this construction could prove that the contact angle uncertainty remains small, thus justifying the mentioned approach for the meniscus. The intermediate zone extent is on the one hand much greater than the microscale (the microstructure), but on the other hand it is still much smaller than the macroscopic radii of curvature such as those of the meniscus and of the wall. The wall curvature, taken into consideration here (albeit in the framework of a planar geometry, neglecting the second curvature), is assumed to vary smoothly on the length scale given by the corresponding radius of curvature, so that it remains constant to leading order on the scales of both the microstructure and the intermediate zone.

The remainder of the paper is organized as follows. In Section 2, the contact line microstructure formulation with a constant slope at infinity is reminded together with the corresponding scales and asymptotics. In Section 3, a formulation with a constant curvature at infinity is rather considered. It also incorporates a constant wall curvature. The interrelation between these two formulations is discussed as appearing in the limit of small curvatures (at infinity and of the wall): small on the microstructure scale, which corresponds to a realistic macroscopic configuration. This opens the way for the intermediate zone treatment in Section 4. Finally, the study is wrapped up in Section 5.

2 Contact line microstructure

Hereafter, we shall use the notation

$$f^* = [f]\, f\,,$$

where f (without asterisk) is the dimensionless version of a dimensional quantity f^* (with asterisk), $[f]$ being the scale.

The nondimensionalization is carried on using the scales of the microstructure (the microscales):

$$[\xi] = \xi_f^*\,,\ [x] = \frac{\xi_f^{*2}}{\sqrt{3}\,a^*}\,,\ a^* = \left(\frac{A^*}{\gamma^*}\right)^{1/2}\,, \qquad (2)$$

where x is the coordinate along the film, a^* is a molecular scale, γ^* is the vapor-liquid surface tension. The ratio of the scales across and along the film

$$\epsilon = \frac{[\xi]}{[x]} = \frac{\sqrt{3}\,a^*}{\xi_f^*}$$

must be small ($\epsilon \ll 1$) both for the macroscopic approach to be valid (requiring $a^* \ll \xi_f^*$) and for the lubrication approximation to be applicable when describing the film dynamics. The curvature scale resulting from (2) is

$$[\kappa] = \frac{[\xi]}{[x]^2} = \frac{\epsilon}{[x]} = \frac{3\,a^{*2}}{\xi_f^{*3}}\,. \qquad (3)$$

The microscales are typically very small, to the extent that the term 'nanoscales' would rather seem more appropriate (yet in the present paper the prefix 'micro'

does not refer to a micrometer scale as such, but is rather used as the opposite to 'macro'). For instance, in the ammonia example [4] at the temperature 300 K and with the superheat $\Delta T = 1\,\mathrm{K}$, one obtains (see also [6]) $a^* = 0.32\,\mathrm{nm}$, $[\xi] = \xi_f^* = 0.95\,\mathrm{nm}$, $[x] = 1.64\,\mathrm{nm}$, $[\kappa]^{-1} = 2.83\,\mathrm{nm}$.

Neglecting for the moment the wall/substrate curvature (which is realistically small on the microstructure scale (3)), and assuming that the superheat nonconstancy along the wall is negligible, the steady lubrication equation for the film thickness can be written as

$$\frac{\partial}{\partial x}\left(\xi^3\,\frac{\partial^3 \xi}{\partial x^3} - \frac{1}{\xi}\,\frac{\partial \xi}{\partial x}\right) + E\,j = 0\,,$$

$$j = \frac{1 - 1/\xi^3 - 3\,\partial^2\xi/\partial x^2}{\xi + K}\,, \qquad (4)$$

where j represents the local evaporation flux, with $[j] = \lambda_l^*\,\Delta T^*/\mathcal{L}^*\xi_f^*$ for the mass flux and $[j] = \lambda_l^*\,\Delta T^*/\xi_f^*$ for the associated heat flux. The dimensionless numbers of the problem are

$$E = \frac{\eta_l^*\,\lambda_l^*\,T_0^*}{3\,a^{*2}\,(\mathcal{L}^*\,\rho_l^*)^2}\,,$$

$$K = \frac{2-\phi}{\phi}\,\sqrt{\frac{\pi\,R_g^*\,T_0^*}{2\,M_w^*}}\,\frac{\lambda_l^*\,T_0^*}{\rho_v^*\,\mathcal{L}^{*2}\,\xi_f^*}\,,$$

For the notations not yet explained, η^* is the dynamic viscosity, λ^* is the heat conductivity, R_g^* is the universal gas constant, M_w^* is the molecular weight, and ϕ is an accommodation coefficient in the evaporation kinetics. In the framework of the one-sided model of an evaporating liquid layer relied upon here, the numerator of j different from unity is due to the Kelvin effect on account of both the disjoining and the Laplace pressures. In the denominator, a term with K is a consequence of accounting for a finite-rate evaporation kinetics ($K = 0$ would correspond to a local phase equilibrium at the interface). E is referred to as the evaporation number, whereas K is the kinetic resistance number. Generally, we imply $E = O(1)$ and $K = O(1)$. In the earlier mentioned ammonia example [4], we have (see also [6]) $\epsilon = 0.58$, $E = 0.124$ and $K = 5.74$. The second example of [7] corresponds to $\epsilon = 0.45$, $E = 7$ and $K = 50$. Up to notations and scaling factors, and excluding additional physical effects sometimes incorporated into the model, equation (4) is of course the same as elsewhere (cf. [4, 7], while for a more detailed presentation in the same terms as here see [6]).

The microfilm boundary condition is

$$\xi = 1 \quad \text{as } x \to -\infty\,. \qquad (5)$$

As one can establish from equation (4), the value $\xi = 1$ is attained exponentially as $x \to -\infty$. Thus, $j \to 0$ also exponentially as $x \to -\infty$. This permits to define another quantity of interest, namely, the integral evaporation flux:

$$J(x) \equiv \int\limits_{-\infty}^{x} j(x')\,dx' = -\frac{1}{E}\,\left(\xi^3\,\frac{\partial^3\xi}{\partial x^3} - \frac{1}{\xi}\,\frac{\partial\xi}{\partial x}\right) \qquad (6)$$

with $[J] = \lambda_l^*\,\Delta T^*/\mathcal{L}^*\epsilon$ for the mass flux and $[J] = \lambda_l^*\,\Delta T^*/\epsilon$ for the associated heat flux. The second equality (6) is derived using (4) and (5).

In the microstructure formulation with a constant slope at infinity (cf. above), the other boundary condition is

$$\xi \sim b\,x \quad \text{as } x \to +\infty\,, \qquad (7)$$

where b is a rescaled contact angle, the true one being

$$\theta = \epsilon\,b\,. \qquad (8)$$

Note that $b = O(1)$, whereas the smallness of the slope required for the lubrication approximation is accounted for by $\epsilon \ll 1$. The rescaled angle $b = b(E, K)$ is a nonlinear eigenvalue of the boundary-value problem (4), (5), (7), an extensive parametric study of which is undertaken in [6].

Using equation (4), one can derive more terms behind the asymptotic behavior (7):

$$\xi \sim b\,(x - x_0) - \frac{E}{4\,b^4}\,\log^2(x/k) + O\left(\frac{\log^3 x}{x}\right)$$

$$\text{as } x \to +\infty\,, \qquad (9)$$

where $k = k(E, K)$ is a well-defined value for the boundary-value problem (4), (5), (7), whereas x_0 just fixes the reference along x and can be chosen arbitrarily (the problem is invariant to shifts along x). In what follows,

$$x_0 \equiv 0\,.$$

The corresponding asymptotic behavior of the integral flux, as one can verify from (6), is

$$J \sim \frac{1}{b}\,\left(\log(x/k) - \frac{3}{2}\right) + O\left(\frac{\log^2 x}{x}\right) \quad \text{as } x \to +\infty\,. \qquad (10)$$

We see that J logarithmically diverges at infinity. More details concerning these asymptotic behaviors are given in [6].

3 Formulation with the curvature

On the other hand, if a given curvature κ_m of the vapor-liquid interface is rather specified towards the macroscopic region (e.g. corresponding to the curvature of the meniscus near the contact line) and if κ_w is the wall curvature (assumed to be constant on the scales involved here), the boundary-value problem for the film thickness ξ becomes

$$\frac{\partial}{\partial x}\left(\xi^3\,\frac{\partial^3\xi}{\partial x^3}-\frac{1}{\xi}\frac{\partial\xi}{\partial x}\right)+E\,j=0\,,$$

$$j=\frac{1-1/\xi^3-3\,\partial^2\xi/\partial x^2-3\,\kappa_w}{\xi+K}\,, \qquad (11)$$

$$\xi=(1-3\,\kappa_w)^{-1/3}\quad\text{as } x\to-\infty\,, \qquad (12)$$

$$\xi\sim\frac{1}{2}\,\kappa\,x^2\quad\text{as } x\to+\infty\,, \qquad (13)$$

where

$$\kappa\equiv\kappa_m-\kappa_w>0 \qquad (14)$$

is assumed to be positive. Note that as written here, the dimensional scale of all the curvature quantities (κ_m, κ_w and κ) is given by (3). Note also that the integral flux expression (6) remains valid for the boundary-value problem (11)-(13). As compared to (4), the change in the numerator of j in (12) reflects the fact that $\partial^2\xi/\partial x^2$ is no longer the free surface curvature to appear in the term representing the Laplace pressure. Now the free surface curvature is rather given by $\partial^2\xi/\partial x^2+\kappa_w$. The thickness of the adsorbed microfilm in (12) changes accordingly as compared to (5).

Again, including more terms in the expansion at infinity, one obtains

$$\xi\sim\frac{1}{2}\,\kappa\,(x-\bar{x}_0)^2+\bar{b}\,(x-\bar{x}_0)+\frac{\bar{C}_{-3}}{x^3}+O\left(\frac{1}{x^4}\right)\quad\text{as } x\to+\infty\,, \qquad (15)$$

where $\bar{b}=\bar{b}(E,K,\kappa,\kappa_w)$ and $\bar{C}_{-3}=\bar{C}_{-3}(E,K,\kappa,\kappa_w)$ in the framework of the problem (11)-(13), whereas $\bar{x}_0$ can be arbitrary. We also note, using (6) with (15), that

$$J(+\infty)=15\,\kappa^3\,\bar{C}_{-3}/(2\,E)\,, \qquad (16)$$

so that with a non-zero curvature the integral flux reaches saturation at infinity, unlike (10).

Below, when speaking about the orders of magnitude, we shall always mean $\kappa_w=O(\kappa)$. For $\kappa=O(1)$, the liquid film configuration to result from the problem (4), (5), (7) and the one to result from (11)-(13) must be distinct and in no particular relation to each other. Nonetheless, in the case $\kappa\ll1$ (as it should be for the macroscopic curvature on the scale of the microstructure, e.g. for $\kappa^*=1\,\mathrm{mm}^{-1}$ we obtain $\kappa\approx2.83\times10^{-6}$ in the framework of the earlier mentioned ammonia example), the former configuration can be conjectured to form part of the latter to leading order while corresponding to not so large values of x (see figure 1). In particular, the behavior (9) should now be recovered as an intermediate asymptotics for large x, but not too large. For these larger x, in what we shall refer to as an intermediate zone, the solution must behave as (9) towards the left end while observing (15) to the right, as $x\to+\infty$. Should the uncertainty in the definition of the contact angle be small as expected, the difference between b and $\bar{b}$ must also be small as $\kappa\to0$. Next, we proceed to analyzing the solution for this intermediate zone, hence confirming these conjectures.

4 Solution in the intermediate zone

The new variables

$$\tilde{x}=\kappa\,x\,,\ \tilde{\xi}=\kappa\,\xi \qquad (17)$$

are introduced, which are positive in view of (14). On account of $\epsilon\ll1$, one can verify that this zone is still much smaller by order of magnitude than the radii of curvature of the meniscus and the wall (the latter being of the order of $\kappa^{-1}\epsilon^{-1}$ on the $[x]$ scale of the microstructure – cf. (2) and (3)). The solution is sought in the form

$$\tilde{\xi}=b\,\tilde{x}+\frac{1}{2}\,\tilde{x}^2+\kappa\,\tilde{\xi}_1\,, \qquad (18)$$

which actually already anticipates the difference between b and $\bar{b}$ being small provided that the appropriate solution exists for $\tilde{\xi}_1$. To leading order, the equation for $\tilde{\xi}_1$ is

$$\frac{\partial}{\partial\tilde{x}}\left[\left(b\,\tilde{x}+\frac{1}{2}\,\tilde{x}^2\right)^3\frac{\partial^3\tilde{\xi}_1}{\partial\tilde{x}^3}\right]+\frac{E}{b\,\tilde{x}+\tilde{x}^2/2}=0$$

with the solution

$$\begin{aligned}\tilde{\xi}_1=\tilde{C}_0+\tilde{C}_1\,\tilde{x}+\tilde{C}_2\,\tilde{x}^2\\+\tilde{C}_3\,\left(2\,b^2+6\,b\,\tilde{x}+3\,\tilde{x}^2\right)\log\frac{\tilde{x}+2\,b}{\tilde{x}}\\+\frac{3\,E}{4\,b^5}\,(\tilde{x}+b)\,\log\frac{\tilde{x}+2\,b}{\tilde{x}}\\-\frac{E}{8\,b^6}\,\left(2\,b^2+6\,b\,\tilde{x}+3\,\tilde{x}^2\right)\log^2\frac{\tilde{x}+2\,b}{\tilde{x}}\,.\end{aligned} \qquad (19)$$

Here by definition all of the macroscopic curvature in the vicinity of the contact line is comprised in κ so that no corrections to it are warranted. Thus,

$$\tilde{C}_2=0\,. \qquad (20)$$

Matching with (9) (formally as $\tilde{x} \to 0$ whereas $x \to +\infty$) yields the expressions for two more coefficients:

$$\tilde{C}_0 = -\frac{E}{4\,b^4}\,\log^2\frac{k\,\kappa}{2\,b}\,,\quad \tilde{C}_3 = -\frac{E}{4\,b^6}\,\left(\frac{3}{2}+\log\frac{k\,\kappa}{2\,b}\right). \tag{21}$$

Nonetheless, to obtain $\tilde{C}_1$, the leading-order solution in the microstructure zone is not enough, and one must consider the first correction in $\kappa \ll 1$ (and $\kappa_w \ll 1$). Let $\xi = \xi_0 + \kappa\,\xi_{11} + \kappa_w\,\xi_{12} + \ldots$, where ξ_0 is just the solution of (4), (5), (7). The corrections ξ_{11} and ξ_{12} satisfy the linearized version of equation (11). The equation for ξ_{11} is homogeneous. The equation for ξ_{12} is inhomogeneous, the homogeneous part being the same as for ξ_{11}, of course. The inhomogeneity originates from the term with κ_w in (11). The equations are omitted here for the sake of brevity, but the boundary conditions are

$$\xi_{11} = 0\,,\ \xi_{12} = 1 \quad \text{as } x \to -\infty\,,$$

$$\xi_{11} \sim \frac{1}{2}\,x^2\,,\ \xi_{12} \sim b_{12}\,x \quad \text{as } x \to +\infty\,,$$

where the latter should be interpreted in terms of matching with the intermediate-zone solution (18). More terms of the large-x expansion for ξ_{11} are

$$\xi_{11} \sim \frac{1}{2}\,x^2 - \frac{3\,E}{4\,b^5}\,x\,\log^2 x + \frac{E}{4\,b^5}\,(7+6\,\log k)\,x\,\log x + b_{11}\,x + O\left(\log^4 x\right) \quad \text{as } x \to +\infty\,. \tag{22}$$

The coefficient $b_{11} = b_{11}(E,K)$ is a well-defined value given by the boundary-value problem for ξ_{11} (as soon as we have fixed $x_0 \equiv 0$ within the leading-order solution $\xi_0(x)$). As for determining b_{12}, no additional computation is in fact needed since one can recur to a mere rescaling. Indeed, the problem (11), (12) with (7) in lieu of (13) can be reduced to (4), (5), (7) by means of the following rescaling:

$$\xi \Rightarrow (1-3\,\kappa_w)^{-1/3}\,\xi\,,\quad x \Rightarrow (1-3\,\kappa_w)^{-2/3}\,x\,,$$

$$b \Rightarrow (1-3\,\kappa_w)^{1/3}\,b\,,\ E \Rightarrow E\,,\ K \Rightarrow (1-3\,\kappa_w)^{-1/3}\,K\,.$$

On account of this, one can see then that b_{12} can be determined using the functional form $b = b(E,K)$ through an appropriate linearization. Thus, one obtains

$$b_{12} = -b(E,K) - K\,\frac{\partial b}{\partial K}(E,K)\,. \tag{23}$$

Now $\tilde{C}_1$ gets determined through matching between (18) with (19) and $\xi = \xi_0 + \kappa\,\xi_{11} + \kappa_w\,\xi_{12}$:

$$\tilde{C}_1 = b_{11} + \frac{\kappa_w}{\kappa}\,b_{12} + \frac{E}{4\,b^5}\left(7\,\log k + 3\,\log^2 k - 6\,\log\frac{k\,\kappa}{2\,b} - 3\,\log^2\frac{k\,\kappa}{2\,b}\right), \tag{24}$$

which finalizes the solution (19), where the parameters have been expressed in terms of the microstructure properties $b = b(E,K)$, $k = k(E,K)$, $b_{11} = b_{11}(E,K)$ and $b_{12} = b_{12}(E,K)$, the latter being expressed by (23).

Calculating the $\tilde{x} \to +\infty$ asymptotics from (18) with (19) and rendering it in the form (15), one obtains

$$\bar{b} - b = \kappa\left[b_{11} + \frac{\kappa_w}{\kappa}\,b_{12} + \frac{E}{4\,b^5}\left(7\,\log k + 3\,\log^2 k - 6\,\log\frac{k\,\kappa}{2\,b} - 2\,\log^2\frac{k\,\kappa}{2\,b}\right)\right], \tag{25}$$

which is seen to remain small for $\kappa \ll 1$ ($\kappa_w = O(\kappa)$). One also obtains

$$\bar{C}_{-3} = \frac{8}{15}\,b^5\tilde{C}_3\kappa^{-3}\,.$$

When used in (16), it yields the value of the integral flux

$$J(+\infty) = -\frac{1}{b}\,\left(\frac{3}{2}+\log\frac{k\,\kappa}{2\,b}\right) \tag{26}$$

which, combined with the values of $b = b(E,K)$ and $k = k(E,K)$ calculated for the microstructure problem [6], allows to evaluate the effect of macroscopic curvature upon J. The result (26) can also be derived in a more elementary way [3]. Indeed, in the original variables x and ξ, the leading-order integral flux throughout the intermediate zone can be written as (cf. (4), (6) with $\xi = b\,x + \kappa\,x^2/2$ corresponding to the first two terms in (18))

$$\int_{x_1}^{+\infty}\frac{dx}{b\,x+\kappa\,x^2/2}\,, \tag{27}$$

where x_1 is a value at the left edge of the zone ($x_1\,\kappa \ll 1$, but $x_1 \gg 1$). Now evaluating the leading-order contribution (10) from the microstructure at this same value $x = x_1$ and summing up with (27), one recovers the result (26).

5 Discussion and concluding remarks

Thus, the solution for the film thickness in the intermediate zone is given by (18) and (19) with (20), (21), (24), where the variables are defined in (17), whereas the original variables x and ξ, as well as the curvatures κ_w (of the wall), κ_m (of the meniscus) and $\kappa \equiv \kappa_m - \kappa_w$, are nondimensionalized using the microstructure scales (2) and (3) with (1). As the macroscopic curvature is small on the microscale, the dimensionless curvature values obtained in this way are all small: $\kappa_w \ll 1$, $\kappa_m \ll 1$, $\kappa \ll 1$. This is in fact one of the premises permitting distinguishing the intermediate zone as such,

with a length scale much greater than that of the microstructure (cf. the rescaling (17)). Another premise is that the apparent contact angle be small (cf. (8) with $\epsilon \ll 1$, $b = O(1)$), so that this (intermediate) length scale is yet much smaller than the radii of curvature of the meniscus and of the wall (cf. figure 1 for the scales). On the one side ($\tilde{x} \to 0$, even though $x \to +\infty$), this intermediate solution matches the microstructure far asymptotics (9). On the other side (meniscus), the asymptotic behavior of the form (15) is recovered. The slope difference between (9) and (15) is given by the result (25) and can be interpreted as the uncertainty in the definition of the (rescaled – cf.(8)) contact angle due to a finite (even though small) macroscopic curvature. The parameters appearing in all these results represent the microstructure properties $b = b(E, K) = O(1)$, $k = k(E, K) = O(1)$, $b_{11} = b_{11}(E, K) = O(1)$ and $b_{12} = b_{12}(E, K) = O(1)$. The first two are obtained from the leading-order problem for the microstructure, given by (4), (5), (7), where note the asymptotic behaviors (9) and (10) which the parameter k is defined through (cf. [6], where an extensive parametric study of this problem is undertaken). The third originates from the first correction ξ_{11} within the microstructure as described in Section 4, with the far asymptotics (22). The fourth one is given by (23) once the functional dependence $b = b(E, K)$ is known.

To the leading order in $\kappa \ll 1$, as one can observe in (18) with (19), it turns out that the solution in the intermediate zone is just trivial: it is a superposition of the leading-order contribution from the adjacent microstructure and meniscus regions. This confirms (and goes along with) the validity of the intuitive approach as described in the abstract. It is only at a higher order (the first correction) that nontrivial, inherently intermediate-zone contributions appear in the solution. As a result, a contact angle uncertainty, equation (25), emerges. But as it belongs to the first correction and not the leading order, it is small, of the relative order $O(\kappa \log^2 \kappa)$. Rather than quantitative, the importance of the correction is first of all in the very fact that it can be constructed, thus validating the degenerate (no contact angle uncertainty) leading-order result. It is noteworthy that the contact angle relative uncertainty is not just $O(\kappa)$, but rather is logarithmically modified. The latter fact lowers the importance of knowing b_{11} (and thus supplementally calculating the first correction in the microstructure region) for the estimation of the uncertainty, equation (25), for it is the logarithmic terms that are expected to dominate therein.

While the integral evaporation flux logarithmically diverges in the microstructure region as specified by (10), it converges in the intermediate zone to a finite value (26) thanks to the effect of macroscopic curvature. Here recall that the dimensional scale of the flux is specified following equation (6). The mere fact of its convergence in the intermediate zone indicates that the corresponding contribution from the remainder of the meniscus is asymptotically smaller (it is expected to be of the order $O(\epsilon)$, cf. [3]). It is noteworthy that the meniscus and wall curvatures (κ_m and κ_w, respectively) enter the results in a combination $\kappa = \kappa_m - \kappa_w$. This does not only concern the expression for the flux, but also the other results for the intermediate zone with the exception of some parts depending on the first correction in the microstructure region where κ_w can appear separately. Note that an equivalent expression for the converged integral flux is obtained by Morris [3], although formally for a flat wall, without the effect of the wall curvature.

Acknowledgements This study has benefited from stimulating discussions with C. Romestant and S. Rossomme. The authors acknowledge financial support of the ESA MAP-BOILING and Belgian PRODEX research programmes, as well as of the Communauté Française de Belgique through the ARCHIMEDES (ARC 04/09-308) project. PC also gratefully acknowledges financial support of the Fonds de la Recherche Scientifique - F.N.R.S.

References

1. M. Potash and P.C. Wayner. Evaporation from a two dimensional extended meniscus. *Int. J. Heat Mass Transfer*, 15:1851–1863, 1972.
2. S. Moosman and G.M. Homsy. Evaporating menisci of wetting fluids. *J. Colloid Interface Sci.*, 73:212–223, 1980.
3. S.J.S. Morris. The evaporating meniscus in a channel. *J. Fluid Mech.*, 494:297–317, 2003.
4. P.C. Stephan and C.A. Busse. Analysis of the heat transfer coefficient of grooved heat pipe evaporator walls. *Int. J. Heat Mass Transfer*, 35:383–391, 1992.
5. S. Rossomme, C. Goffaux, K. Hillewaert, and P. Colinet. Multi-scale numerical modeling of radial heat transfer in grooved heat pipes. *Microgravity Sci. Technol.*, 20:293–297, 2008.
6. A.Ye. Rednikov, S. Rossomme, and P. Colinet. Steady microstructure of a contact line for a liquid on a heated surface overlaid with its pure vapor: parametric study for a classical model. *Multiphase Sci. Technol.*, 21:213–248, 2009.
7. S.J.S. Morris. Contact angles for evaporating liquids predicted and compared with existing experiments. *J. Fluid Mech.*, 432:1–30, 2001.